Growth mechanism of ordered stress-induced patterns in Al films deposited on silicone oil surfaces

2004 J. Phys.: Condens. Matter 16 L147

(http://iopscience.iop.org/0953-8984/16/10/L05)

INSTITUTE OF PHYSICS PUBLISHING JOURNAL OF PHYSICS: CONDENSED MATTER

J. Phys.: Condens. Matter **16** (2004) L147–L154 PII: S0953-8984(04)71187-X

LETTER TO THE EDITOR

Growth mechanism of ordered stress-induced patterns in Al films deposited on silicone oil surfaces

Sen-Jiang Yu[1], Yong-Ju Zhang[1,2], Ping-Gen Cai[1], Quan-Lin Ye[1], Xiao-Wei Tang[1] and Gao-Xiang Ye[1,3]

[1] Department of Physics, Zhejiang University, Hangzhou 310027, People's Republic of China
[2] Department of Physics, Taizhou University, Linhai 317000, People's Republic of China

E-mail: gxye@mail.hz.zj.cn

Received 27 October 2003, in final form 13 February 2004
Published 27 February 2004
Online at stacks.iop.org/JPhysCM/16/L147 (DOI: 10.1088/0953-8984/16/10/L05)

Abstract

An optical microscope study of large spatially ordered patterns in an aluminium (Al) film system deposited on silicone oil surfaces is presented in this letter. The ordered patterns, namely bands, are composed of a large number of rectangle-shaped domains, which are evolved from small triangle-shaped domains with size less than 1 μm in vacuum conditions. The bands start from the film edge and then extend towards the central region of the sample. Both the length and width of the rectangle-shaped domains in each band decrease approximately linearly as the band extends. It is pointed out that the appearance of the bands represents the distribution of the internal stress in the Al films. The theoretical analysis shows that due to the characteristic boundary condition and interactions between the metallic films and the liquid substrates, the nearly free sustained Al films may contain a series of sinusoidal stress distributions with different amplitudes and frequencies, and their composition results in the formation of the ordered stress-induced patterns.

Residual internal stress is an intrinsic property of thin films deposited on various substrates. It plays an important role in determining and controlling the microstructures, surface morphologies and physical properties of the films. Many previous works have reported that beautiful patterns or fascinating structures always emerge in thin film systems deposited on solid, soft polymer and liquid substrates, in which the internal stress is shown to be the driving force for self-organization [1–9]. The typical patterns include large varieties of forms such as one-dimensional (1D) nanowires (or nanotubes) and two- or three-dimensional (2D or 3D) islands on semiconductor surfaces [1–3], periodic surface waves in compressed metallic films on soft polymer substrates [4, 5], undulating buckles in diamond-like carbon (DLC)

[3] Author to whom any correspondence should be addressed.

films [6, 7], sinusoidal cracks in nearly free standing metallic films [8] and characteristic wrinkles in different film/substrate samples [9]. Recently, Ye and co-workers have reported a totally new form of ordered patterns existing in an iron (Fe) film system deposited on silicone oil surfaces [10, 11]. These ordered patterns are composed of a large number of parallel rectangle-shaped domains. It has been proved that the ordered patterns do not relate to the magnetic interactions among the iron atoms (or clusters) and they originate from spontaneous material organization owing to the relaxation of the internal stress after deposition. However, in order to control and possibly tune the pattern formation in this or other similar cases, a deeper understanding of the growth process of the patterns is essential and necessary.

In this letter, we present the main features of the growth mechanism of these stress-induced patterns in continuous aluminium (Al) films deposited on silicone oil surfaces. The experimental results show that the patterns grow successively in vacuum conditions and, once the samples are removed from the vacuum chamber, the growth process stops immediately. Therefore, the growth mechanism of these patterns can be understood with the aid of experiments comparing different growth periods, deposition rates, and film thicknesses. Generally, the patterns can reach a lateral size of 100 μm, which makes it possible to use optical microscopy to follow the growth and the evolution in detail.

The samples were prepared by thermal evaporation of 99.999% pure Al in a vacuum of 6×10^{-4} Pa at room temperature. Commercial silicone oil (Dow Corning 705 diffusion pump fluid) with a vapour pressure below 10^{-8} Pa was painted onto a frosted glass surface, which was fixed 120 mm below the filament (tungsten). The resulting oil substrate with an area of about 10×10 mm^2 had a uniform thickness of $\approx$0.5 mm. In fact, in the oil thickness range of 0.2–0.8 mm, no obvious change of the surface morphologies of the Al films can be observed in our experiment. The deposition rate f and the nominal film thickness d were determined by a quartz-crystal balance, which was calibrated by a profilometer (α-step 200 profilometer, Tencor). After deposition, the sample was kept in the vacuum chamber (in vacuum conditions) for time Δt and then removed from the chamber. All images for the surface morphologies of the samples were taken with an optical microscope (Leica DMLM), equipped with a CCD camera (Leica DC 300) which was interfaced to a computer for data storage and data processing.

Figure 1 shows the surface morphologies of two samples, in which the Al film edges and ordered patterns are observed. In figure 1(c), the ordered patterns, namely bands, are shown at a higher resolution, so that more details of the bands become observable. We find that each band is in fact a broken dark line, and according to the photos taken by the optical microscope the broken dark lines are cracks in the film. In each band, rectangular structures, namely keys, can be observed clearly, although one side of each key is open. In other words, the broken dark line is the boundaries of all the parallel keys or domains. Generally, the neighbouring keys in each band possess different widths w but nearly uniform length L (see figure 1(c)), and therefore the bands possess a quasi-periodic structure. The experiment shows that the bands extend from the film edges towards the central regions of the samples over various distances (figure 1). In some cases, the band may start at one film edge and end at the opposite edge of the sample, and the total length of the band may be more than 10 mm. The black arrows in figure 1(c) denote the typical morphologies of the bands in the film regions where the bands start and end. When the bands extend, they may undergo a gradual and slight change in their propagation directions and all the bands starting at the same film edge extend in approximately the same direction (see figure 1), indicating that there is a strong orientation to the growth of the bands in the vicinity of the film edge. In addition, our experiment shows that the morphologies of the bands on the bottom surface of the Al film, i.e., the surface in contact with the oil substrate during deposition, are similar to those of the bands on the top surface, providing evidence that the bands are an ordered bulk structure.

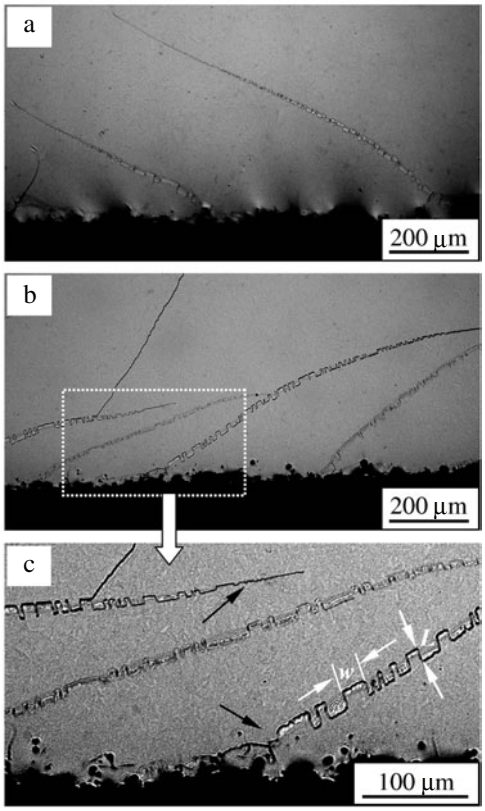

Figure 1. Surface morphologies of two Al films deposited on silicone oil surfaces. (a) $f = 0.10$ nm s^{-1}, $d = 30$ nm, $\Delta t = 0.5$ h; (b) $f = 0.16$ nm s^{-1}, $d = 20$ nm, $\Delta t = 0.5$ h; (c) the ordered patterns in (b) shown at a higher magnification.

Another interesting phenomenon in figure 1 is that the key length L and key width w always decrease obviously as the bands extend. In order to describe the extension behaviour of the bands quantitatively, for the samples with different nominal film thicknesses we measured the length L and the average key width $\overline{w}$ with the extension distance ξ. The corresponding results are shown in figures 2(a) and (b), respectively. We find that, to a good approximation, the length L and average width $\overline{w}$ both decay linearly with the distance ξ, which can be expressed as

$$L = L_0 - \gamma\xi \tag{1}$$

and

$$\overline{w} = \overline{w}_0 - \beta\xi, \tag{2}$$

where L_0 and $\overline{w}_0$ are the maximum values of L and $\overline{w}$, respectively. According to our experiment, the linear decay behaviour equation (2) is apparent for all the samples if the average width $\overline{w}$ is counted from more than ten neighbouring keys.

In the nominal film thickness range of $d = 10$–120 nm, all the measurements show that the linear fit slopes, i.e., γ and β, which represent the attenuation rates of the key length and width with the distance ξ, increase obviously with the nominal film thickness d (see figure 2). It can also be seen from figure 2 that L_0 and $\overline{w}_0$ change clearly when d increases.

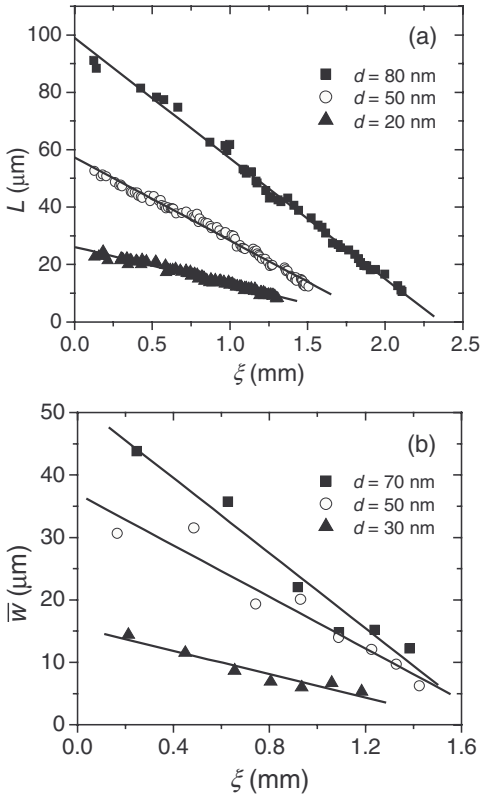

Figure 2. (a) Evolution of the key length L with the extension distance ξ. (b) Evolution of the average key width $\overline{w}$ with ξ. Each data point of $\overline{w}$ represents an average value of over ten neighbouring keys. The solid lines are linear fits to the experimental data. $f = 0.11$ nm s^{-1}, $\Delta t = 0.5$ h.

Further experimental studies show that both L_0 and $\overline{w}_0$ first increase drastically and then decrease steadily with increasing nominal film thickness. In the range of $d = 70$–80 nm, L_0 and $\overline{w}_0$ reach their maximum values of about 110 and 70 μm, respectively.

In addition, our experiment shows that once the band forms, the width w is settled. Therefore, the average width $\overline{w}$, maximum value $\overline{w}_0$ and attenuation rate β should remain unchanged when the time Δt increases. In order to further understand the extension behaviour of the bands in vacuum conditions, we systematically measured the maximum key length L_0 and the attenuation rate γ with the time Δt, and the results are shown in figure 3(a). One finds that L_0 increases rapidly with Δt first, then its growth speed slows down and finally L_0 approaches a saturated value. The obvious growth period of the key length, depending on the nominal film thickness, is of the order of several hours in our experiment [10–14]. However, although the length L increases obviously in vacuum conditions, γ is almost independent of the time Δt (see figure 3(a)), which indicates that all keys in each band may grow with a nearly uniform speed.

Based on the description above, the extension behaviour of the bands can be sketched vividly, as shown in figure 3(b). After deposition, as the time Δt increases, the bands extend from the film edge to the central region of the sample gradually. During this process, in each band both the key length L and the total length of the band increase simultaneously and the

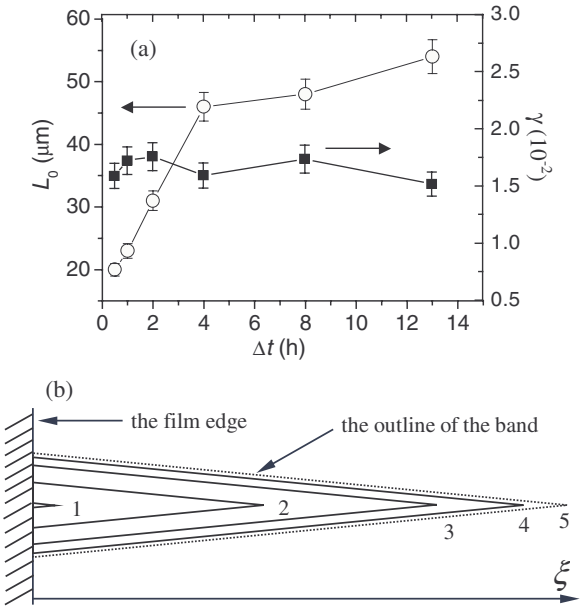

Figure 3. (a) Maximum key length L_0 and attenuation rate γ as functions of the time Δt. The solid lines between the data points are guides to the eye. $f = 0.11$ nm s^{-1}, $d = 20$ nm. (b) Schematic drawing of the extension process of the band in vacuum conditions. When the time Δt increases, the band grows from outline 1 to 5 gradually.

band grows successively from outline 1 to 5 shown in figure 3(b). Since all the keys in the band grow with a nearly uniform speed, the outline of the band may exhibit a series of similar triangles with different sizes. Our experiment shows that the extension of the band is faster at the beginning and then slows down gradually. Several hours later, the growth of the band stops and it reaches a stable state (see the dashed lines in figure 3(b)).

According to the experimental observations, the appearance of the keys depends on the time Δt, deposition rate f, nominal film thickness d and distance ξ. If $\Delta t = 0.5$ h, in the ranges of $f \approx 0.05$–0.35 nm s^{-1} and $d \approx 10$–120 nm, the rectangular keys with different L and w, as shown in figure 1, can be observed in all the bands. For the samples with $d \approx 5$–10 nm, however, the appearance of the keys changes obviously as the bands extend. Figure 4 shows the typical morphological evolution of a band with the distance ξ, in which the rectangular keys appear near the film edge (figure 4(a)), while small triangle-shaped domains form at the end of the band (figure 4(d)). According to the intrinsic extension behaviour of the bands shown in figure 3(b), the domains near the film edge form earlier than those in the central region of the sample, which gives information that the rectangular keys may be evolved from the small triangle-shaped domains. This conclusion has been confirmed in our experiment by comparing the samples with different time Δt.

Based on the experimental observations above, the formation of the bands can be traced to a three-stage process. Firstly, after the continuous Al film forms, strips with a characteristic domain structure (see the black arrows in figure 4) appear near the film edge and extend to the central region of the sample gradually. In the subsequent stage, small triangle-shaped domains start to appear in the strip (figure 4(d)) and they grow successively until they connect with each other (figure 4(c)). Lastly, the domains grow steadily in the directions perpendicular to the strip (figures 4(a) and (b)), which finally results in the formation of the rectangular keys

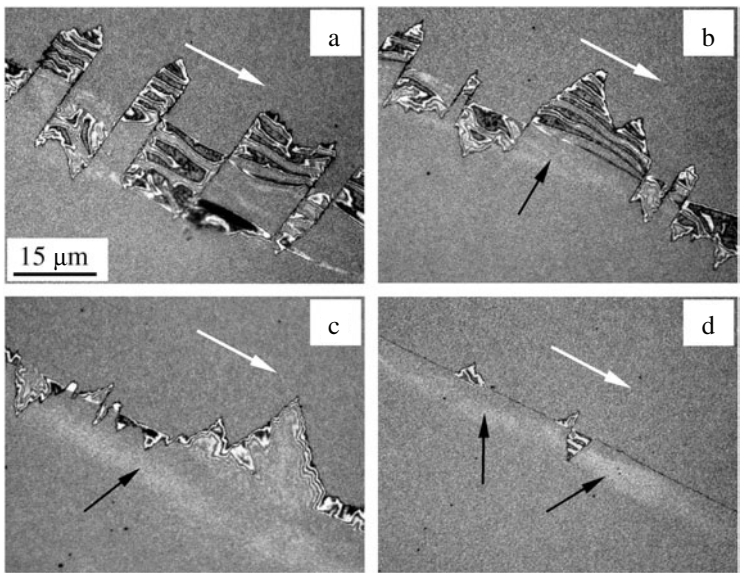

Figure 4. Morphological evolution of a band with the distance ξ. The white arrows denote the propagation direction of the band and the black arrows mark the strip with a characteristic domain structure. (a) $\xi = 0.1$ mm; (b) $\xi = 0.3$ mm; (c) $\xi = 0.7$ mm; (d) $\xi = 1.3$ mm. $f = 0.10$ nm s^{-1}, $d = 8$ nm, $\Delta t = 2.5$ h. Each image has a size of 65×50 μm^2.

and the band with a quasi-periodic structure, as shown in figure 1. Our experiment shows that the larger the nominal film thickness d is, the earlier the rectangular keys would form. For instance, the formation periods of the rectangular keys in two Al samples with $d = 10$ and 8 nm are about 0.5 and 2.5 h, respectively.

According to the previous studies [8–11], strong and detectable residual internal stress always exists in metallic films deposited on liquid substrates and characteristic stress-induced surface morphologies can be observed in these nearly free sustained films. We believe that the Al films and the silicone oil substrates both expand during deposition owing to the heat radiation from the filament [9]. In the subsequent cooling process, the contraction behaviours of the films and the substrates result in the detectable residual internal stress, which may be relieved by the spontaneous formation of the bands. The residual internal stress distributions in the film edges should be different from those in the central regions of the samples since their boundary conditions are not alike [4, 5], which finally results in the phenomenon that the bands extend from the film edges to the central regions of the samples. The appearance of the bands generally represents the distribution of the internal stress because the favourable direction in which the stress-induced patterns extend is always perpendicular to the axis of the highest stress, which enables greatest stress energy release [4–7].

Several works have attempted to theoretically understand the stress-induced patterns in thin films [4–8]. The validity of the models put forward using the general theory of buckling of plates and the buckling equation is given by [6]

$$D\left(\frac{\partial^4 W}{\partial x^4} + 2\frac{\partial^4 W}{\partial x^2 \partial y^2} + \frac{\partial^4 W}{\partial y^4}\right) + \sigma_x d\,\frac{\partial^2 W}{\partial x^2} + \sigma_y d\,\frac{\partial^2 W}{\partial y^2} + 2\tau_{xy} d\,\frac{\partial^2 W}{\partial x \partial y} + F = 0, \tag{3}$$

where D is the moment of inertia of the film, d is the film thickness, x and y are the coordinates relative to the substrate, W is the film coordinate as defined in the elastic theory, σ_x and σ_y are the internal compressive stresses, τ_{xy} is the shear stress and F is the external force.

One type of solution of equation (3) which is physically acceptable is [6]

$$W = 1 + \cos(kx + qy). \tag{4}$$

This solution implies that the film buckling perpendicular to the direction of the highest stress is along a straight line given by

$$kx + qy = 2n\pi, \qquad n = 0, \pm 1, \pm 2, \ldots. \tag{5}$$

Introducing equation (4) into (3) shows that for each k value there are two permissible values of q, and therefore the solution of equation (5) consists of two classes of parallel line families with slopes of $\pm|k/q|$, which cross each other [6]. Many stress-induced patterns can be well explained by making use of this model. For example, if a propagating buckle reaches a point where two lines cross each other, it jumps from one line to the other with different slope and this process may result in the sinusoidal pattern [6–8].

It is clear that a pair of values of k and q corresponds to a kind of distribution of the internal stress. In fact, the values of k and q are not unique and equation (3) can be satisfied by different real values of k and q (see equations (4) and (5)), which means that many kinds of sinusoidal (or cosine) stress distribution can exist simultaneously in each film. According to the Fourier transform principle, each characteristic appearance of the keys shows a corresponding spatial frequency spectrum of the stress pattern and the evolution of the keys' appearance with Δt represents the relaxation behaviour of the stress in the films. The experimental results shown in figures 1 and 4 indicate that the frequency spectra of the stress distributions in the nearly free sustained Al films are quite plentiful and evolve with Δt. In other words, the composition of the various sinusoidal stress patterns with different periods, phases and amplitudes results in the formation of the keys and then the bands shown in figures 1 and 4.

Based on the results shown in figures 1–4, the frequency spectra of the stress distributions in the Al films are location dependent. The phenomenon shown in figure 4 gives evidence that the composition of the various sinusoidal stress distributions can result in triangle-shaped or rectangle-shaped stress distributions, which correspond to the triangle-shaped domains and rectangular keys, respectively. The characteristic forms of the internal stress distributions strongly depend on the location in the film. Generally, the internal stress distributions exhibit rectangle-shaped forms near the film edge, and they may evolve into triangle-shaped forms gradually when the distance ξ increases. Furthermore, the oscillatory amplitudes of the internal stress distributions may decrease and their oscillatory frequencies may increase with the distance ξ, which leads to the experimental results that both the length L and width w decrease obviously as the bands extend from the film edge to the central region of the sample, as shown in figures 1, 2 and 4.

On the other hand, it has been proved above that the rectangular keys are evolved from the small triangle-shaped domains with the size less than 1 μm in vacuum conditions, giving evidence that the frequency spectra of the stress distributions in the Al films strongly depend on the time Δt. After deposition, when Δt increases, the triangle-shaped stress distributions form in the Al film first, then they evolve into the rectangle-shaped stress distributions gradually and, in this period, the width w keeps unchanged and the length L increases obviously (figure 3(a)). Therefore, after the rectangle-shaped stress distributions form, the oscillatory frequencies are settled, while the oscillatory amplitudes increase successively with the time Δt until the internal stress in the Al film relaxes completely.

In a word, the frequency spectra of the stress distributions are not fixed; they are location dependent and may evolve with the time Δt, which results in the nucleation, growth and extension behaviours of the bands in the Al films, as shown in figures 1–4. We believe that the plentiful frequency spectra and the intrinsic growth behaviours of the bands in the Al films strongly relate to the characteristic effect of the liquid substrates since such a kind of

band-shaped structure has never been observed in other film systems on solid or soft polymer substrates. Based on the description above, we propose that the characteristic internal stress distributions in this nearly free sustained Al film system mainly result from the characteristic boundary condition and interactions between the metallic films and the liquid substrates.

The phenomena shown in this letter present us with an example that the films deposited on liquid substrates may possess rather distinctive internal stress distributions, which may in principle result in characteristic microstructures and subsequently anomalous physical properties of the films. However, up to now, the details of the characteristic boundary effect and interactions between the films and the liquid substrates, which should be responsible for the film microstructures and the quasi-periodic ordered patterns, still remain poorly understood. Therefore, further experimental and theoretical studies on these nearly free sustained metallic film systems are still needed.

This work was supported by the National Natural Science Foundation of China (grant No 10174063) and by the Natural Science Foundation of Zhejiang Province in China (grant No 1997-RC9603).

References

[1] Brune H, Giovannini M, Bromann K and Kern K 1998 *Nature* **394** 451
[2] Li A, Liu F, Petrovykh D Y, Lin J L, Viernow J, Himpsel F J and Lagally M G 2000 *Phys. Rev. Lett.* **85** 5380
[3] Owen J H G, Miki K, Koh H, Yeom H W and Bowler D R 2002 *Phys. Rev. Lett.* **88** 226104
[4] Bowden N, Brittain S, Evans A G, Hutchinson J W and Whitesides G M 1998 *Nature* **393** 146
[5] Huck W T S, Bowden N, Onck P, Pardoen T, Hutchinson J W and Whitesides G M 2000 *Langmuir* **16** 3497
[6] Nir D 1984 *Thin Solid Films* **112** 41
[7] Iyer S B, Harshavardhan K S and Kumar V 1995 *Thin Solid Films* **256** 94
[8] Cai P G, Yu S J, Ye Q L, Jin J S and Ye G X 2003 *Phys. Lett.* A **312** 119
[9] Ye G X, Zhang Q R, Feng C M, Ge H L and Jiao Z K 1996 *Phys. Rev.* B **54** 14754
[10] Ye Q L, Yu S J, Jin J S and Ye G X 2003 *Chin. Phys. Lett.* **20** 1109
[11] Ye Q L, Xu X J, Cai P G, Xia A G and Ye G X 2003 *Phys. Lett.* A **318** 457
[12] Ye G X, Michely Th, Weidenhof V, Friedrich I and Wuttig M 1998 *Phys. Rev. Lett.* **81** 622
[13] Yang B, Scheidtmann J, Mayer J, Wuttig M and Michely Th 2002 *Surf. Sci.* **497** 100
[14] Yang B, Xia A G, Jin J S, Ye Q L, Lao Y F, Jiao Z K and Ye G X 2002 *J. Phys.: Condens. Matter* **14** 10051